Dyuti Prakash Sarkar, Jun-ichi Ando, Gautam Ghosh, Kaushik Das, Prabir Dasgupta, and Naotaka Tomioka, 2022, Fault zone architecture and lithology-dependent deformation mechanisms of the Himalayan frontal fold-thrust belt: Insights from the Nahan Thrust, India: GSA Bulletin, https://doi.org/10.1130/B36246.1.

Supplemental Material

Figure S1. Samples from the fault core. (A–B) represent the preserved brecciated blocks. The grain size along the fractured zones is indicated by a red arrow in (A). Fragmented calcite veins marked with red arrows are shown in (B). (C) The sample from the red gouge layer shows fractured clasts with zones of grain-size fining, shown by the red arrow. (D) The sample from the black gouge layer exhibits steep northeast-dipping Y shear planes and moderately northeast-dipping R_1 shear planes (arrows), suggesting a reverse or top-to-southwest sense of shear.

Figure S2. X-ray diffraction patterns of undeformed and fault core rocks. (A) Sandstone (PJ01), gray gouge (PJ5b), and black gouge (PJ5c) showed similar mineral peaks in the >2 μm grain fraction. The finer fractions of the gouges show a reduction in mineral peaks due to the possible decomposition of constituent minerals. (B) Argillaceous sandstone (PJ4) and red gouge (PJ5d) show similar mineral peaks in all grain fractions.

Figure S3. (A) Backscattered electron image showing the elemental mapping area of the ultrafine band and adjacent area. (B–F) Elemental maps using Electron dispersive spectroscopy, and representing abundance as the relative intensities of the corresponding colors. (B) The Si abundance map showing the presence of quartz clasts. (C) The Al abundance map with a higher intensity indicates the abundance of Al-bearing clay minerals in the ultrafine band. Additionally, Al in adjacent areas showed the presence of Al-bearing clay minerals in the matrix. (D) Ca abundance map showing the presence of calcite in adjacent areas but not in ultrafine bands. (E) Mg abundance map showing the absence of Mg-rich phases, except for a component of clay minerals in the matrix. (F) Fe abundance map showing the presence of Fe, possibly only as a component of the clay minerals in the matrix.

Table S1. Centrifugation parameters for grain size fractionation of samples for x-ray diffraction analysis.

Table S2. Representative electron probe micro analyzer data.

Table S3. GPS locations (WGS84) of sample collection points.

DR Figure 1

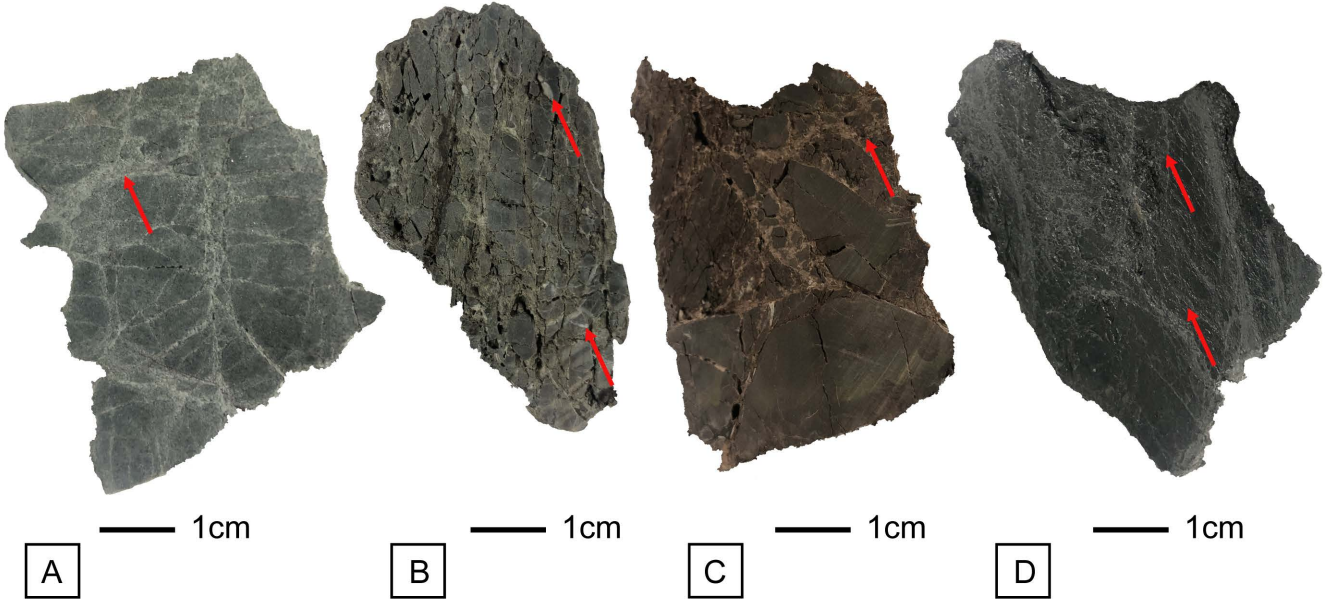

DR Figure 2

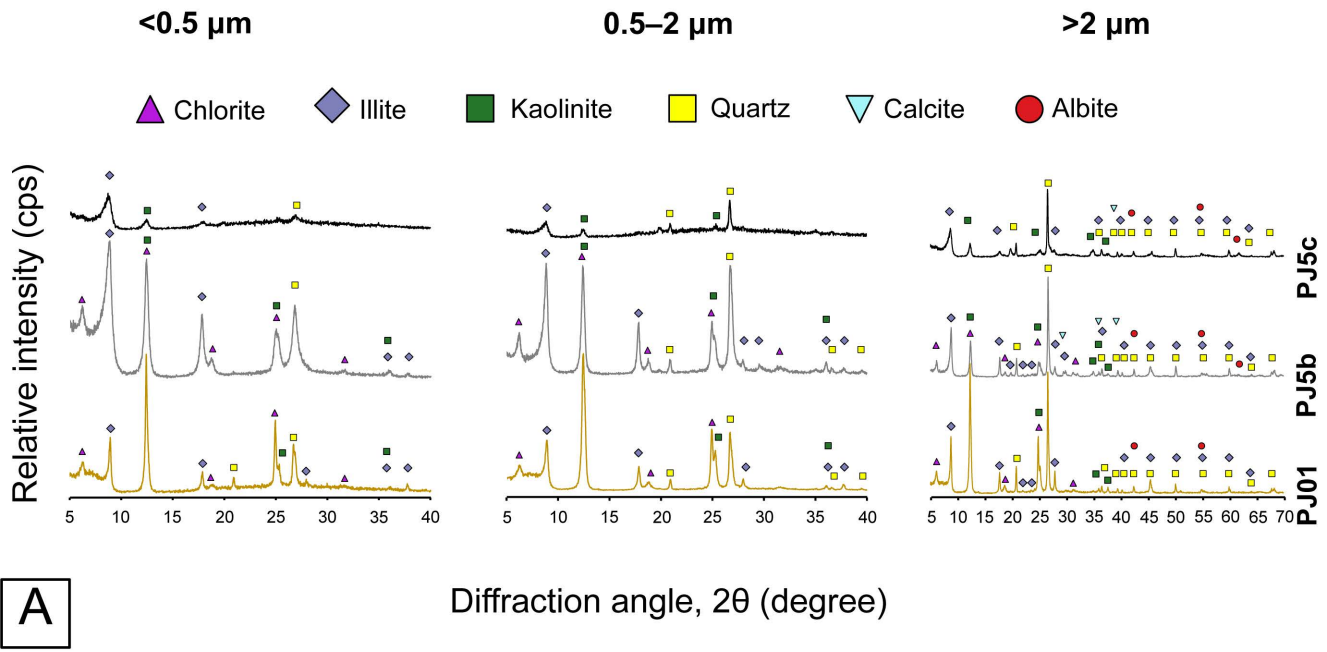
A
<0.5 μm
0.5–2 μm
>2 μm
Chlorite
Illite
Kaolinite
Quartz
Calcite
Albite
Relative intensity (cps)
PJ5c
PJ5b
PJ01
5 10 15 20 25 30 35 40
5 10 15 20 25 30 35 40 45 50 55 60 65 70
Diffraction angle, 2θ (degree)

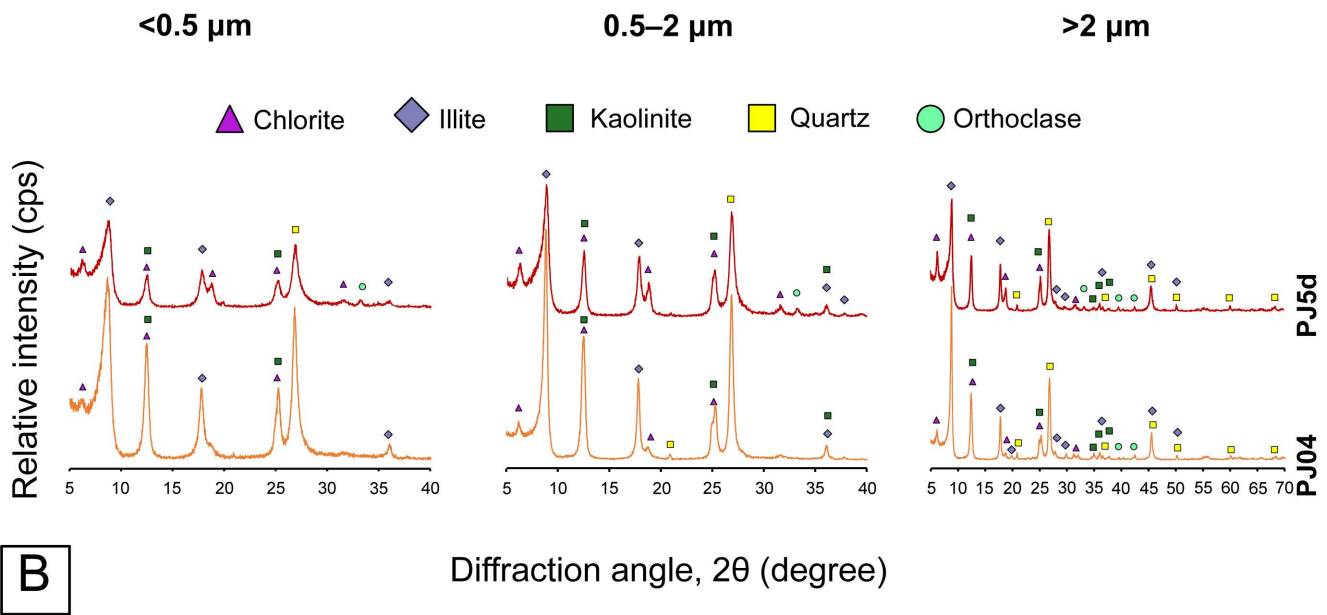
B
<0.5 μm
0.5–2 μm
>2 μm
Chlorite
Illite
Kaolinite
Quartz
Orthoclase
Relative intensity (cps)
PJ5d
PJ04
5 10 15 20 25 30 35 40
5 10 15 20 25 30 35 40 45 50 55 60 65 70
Diffraction angle, 2θ (degree)

DR Figure 3